# Dalton Transactions



## COMMUNICATION

5

10

15

25

40

10

Phthalocyanine-polyoxotungstate lanthanide double deckers†

Cite this: DOI: 10.1039/d0dt03716h

Q2

15

30

35

40

45

Received 28th October 2020, Accepted 3rd November 2020

DOI: 10.1039/d0dt03716h

Sidra Sarwar, a,b Sergio Sanz, b,c Jan van Leusen, a Gary S. Nichol, a Euan K. Brechin and Paul Kögerler a,b,c

rsc.li/dalton

Acetate ligand metathesis results in the first hybrid [M<sup>III</sup>(Pc) (PW<sub>11</sub>O<sub>39</sub>)]<sup>6-</sup> (M = Y, Dy, Tb) double-decker scaffolds, where a phthalocyanate (Pc<sup>2-</sup>) and one of the conceptually most simple polyoxotungstates, a monolacunary Keggin cluster, are interlinked via a single rare earth ion. Characterisation included high-resolution mass spectrometry, synchrotron-based single-crystal X-ray diffraction, various spectroscopic and electrochemical methods, and magnetic studies revealing slow relaxation of the magnetisation for the Dy derivate.

Single-molecule magnets (SMMs), characterised by magnetic bi-stability due to a finite spin ground state and a negative axial zero-field ground state splitting, 1,2 continue to raise interest in the context of quantum computation and molecular spintronics.<sup>3-9</sup> Here, rare earth spin centres are specifically targeted due to their large intrinsic magnetic anisotropy arising from the near degeneracy of the 4f orbitals. 10,11 They offer a key advantage in that and, through careful ligand field design, it is possible to manipulate the magnitude and alignment of anisotropy axes. 12-14 Following this strategy, sandwich-type complexes based on late rare earth metals with phthalocyanine (and other high-symmetry aromatic) ligands have shown great promise as SMM architectures by harnessing 4f single-ion anisotropy. 15-19 The synthesis of homoleptic and heteroleptic double-decker complexes with phthalocyanine ligands has been extensively explored, with significant changes observed in magnetic properties upon chemical modification of peri-

<sup>a</sup>Institute of Inorganic Chemistry, RWTH Aachen University, 52056 Aachen, Germany <sup>b</sup>Peter Grünberg Institute, Electronic Properties (PGI-6), Forschungszentrum Jülich, 52425 lülich. Germany

<sup>c</sup>Jülich-Aachen Research Alliance, Fundamentals for Future Information Technology (JARA-FIT), Forschungszentrum Jülich, 52425 Jülich, Germany

<sup>d</sup>EaStCHEM School of Chemistry, The University of Edinburgh, David Brewster Road, Edinburgh, EH9 3FJ, UK

† Electronic supplementary information (ESI) available: Synthetic description, characterisation and additional figures related to the discussion of results. CCDC 1993274 and 1993275. For ESI and crystallographic data in CIF or other electronic format see DOI: 10.1039/d0dt03716h

pheral substituents. 20-25 To a lesser extent, synthetic chemists have explored replacing one of the phthalocyanine ligands with a polydentate ligand to impose structural changes associated with the chemical and physical properties of the new ligands. Examples include Schiff bases, porphyrins and organometallic tripodal ligands.<sup>26-33</sup> Note that even the replacement of some pyrrole units in the macrocyclic framework with e.g. furan or thiophene, result in a significant change in the magnetic characteristics.<sup>34</sup> On the other hand, redox-active lacunary polyoxometalates act as versatile polydentate ligands towards oxophilic lanthanide ions, resulting in application potentials in electrochemistry, photochemistry, catalysis and magnetism.35-45 Despite these prospects, there is just one report of a double-decker Ln<sup>III</sup> complex comprising both a phthalocyanine and a polyoxometalate, namely a Yb3+ complex with a polyoxovanadate.46 In contrast, we here focus on the lanthanide ions Tb<sup>3+</sup> (4f<sup>8</sup>) and Dy<sup>3+</sup> (4f<sup>9</sup>) that exhibit especially high magnetic anisotropy in LnPc2-type double decker complexes, 15 in conjunction with a thermodynamically highly stable, classical polyoxotungstate ligand.

Herein, we describe the synthesis and characterisation of a new class of Ln double-decker species isolated as  $(N(nBu)_4)_4H_2[M^{III}Pc(PW_{11}O_{39})]$  with M = Y (1), Dy (2) or Tb (3) that contain a Pc<sup>2-</sup> and a monolacunary α-Keggin  $([P^VW^{VI}_{11}O_{39}]^{7-})$  ligand. Key to these syntheses is the precursor [M(Pc)(OAc)], which is reacted with  $(N(nBu)_4)_4H_3[PW_{11}O_{39}]$ ,  $N(nBu)_4Br$ and  $NEt_3$  in a 1:1:1 CH<sub>3</sub>CN: MeOH: CH<sub>2</sub>Cl<sub>2</sub> overnight at 50 °C. The resulting solution is filtered and the mother liquor evaporated to dryness. Precipitation of the dissolved crude material in CH<sub>2</sub>Cl<sub>2</sub> with hexane renders a green powder, which is purified by column chromatography. We started with the diamagnetic analogue,  $[Y^{III}(Pc)(PW_{11}O_{39})]^{6-}$ , to examine its solution behaviour via <sup>1</sup>H and <sup>31</sup>P NMR. Thereafter, 2 and 3 were isolated from similar synthetic procedures, with green rod-like crystals of 3 grown through slow evaporation of a CH<sub>2</sub>Cl<sub>2</sub> solution.

The  $^{1}$ H NMR (600 MHz, CD<sub>3</sub>CN) spectrum of [Y<sup>III</sup>(Pc) (PW<sub>11</sub>O<sub>39</sub>)]<sup>6-</sup>presents broad singlets for H<sub> $\alpha$ </sub> (9.61–9.20 ppm)

Q1

Communication Dalton Transactions

and H<sub>B</sub> (8.34-8.05 ppm) of the Pc ligand, characteristic of a reduced symmetry in the complex (Fig. S12†). While a shift of  $H_{\alpha}$  from ca. 9.42 to 9.50 ppm is observed when the singledecker phthalocyanate complex [YPc(OAc)] coordinates to  $[PW_{11}O_{39}]^{7-}$ ,  $H_{\beta}$  remains relatively unchanged. The <sup>31</sup>P NMR (243 MHz, CD<sub>3</sub>CN) spectrum shows a shift from -13.24 to -14.64 ppm of the  $[PW_{11}O_{39}]^{7-}$  precursor (Fig. S10 and 13†). NMR, EA, IR, UV-Vis, and ESI HRMS are consistent with the purity of the diamagnetic analogue and support the existence of the counteraction composition in 1. Subsequently, compounds 2 and 3 were synthesised and characterised by ESI-HRMS, IR, UV-Vis, and EA. Akin to the Y complex (see ESI† for crystallography information), green rod-like crystals of 3 were obtained from a concentrated CH2Cl2 solution. Several attempts to obtain single crystals of 2 using different mixtures of solvents, cation exchange and crystallisation conditions failed. Both 1 and 3‡ crystallise in a monoclinic system and structure solution was performed in the  $P2_1/c$  and C2/m space groups, respectively. The molecular {MPc(PW<sub>11</sub>O<sub>39</sub>)} units in 1 and 3 are virtually isostructural, and in the following we discuss the representative structure 3.  $[PW_{11}O_{39}]^{7-}$ , the monolacunary derivative of the seminal α-Keggin-type polyanion  $[PW_{12}O_{40}]^{3-}$ , contains a central phosphate 1.478–1.547 Å), coordinating to 11 W<sup>VI</sup> ions *via* three  $\mu_3$ -O and one  $\mu_2$ -O<sub>P</sub> sites (W-O: 2.390-2.498 Å). On the periphery, the  $W^{VI}$  ions are linked by  $\mu_2$ - $O^{2-}$  ions (W-O: 1.792-2.077 Å), with the remaining coordination sites completed by terminal oxo groups (W-O: 1.684-1.704 Å). The defect (lacuna) site of  $[PW_{11}O_{39}]^{7-}$  is defined by four basic oxygen atoms (O···O: 2.81-2.94 Å) that coordinate to the TbPc unit and generate [Tb<sup>III</sup>(Pc)(PW<sub>11</sub>O<sub>39</sub>)]<sup>6-</sup> with Tb<sup>III</sup> adopting a distorted squareantiprismatic N<sub>4</sub>O<sub>4</sub> environment (Tb-O: 2.361 and 2.389 Å; Tb-N: 2.452, 2.465 and 2.467 Å). The TbN<sub>4</sub>O<sub>4</sub> fragment is rotated by a skew angle of 46.08° and 44.44° relative to an eclipsed geometry. The symmetry plane of the  $C_s$ -symmetric  $\{PW_{11}\}\$  unit approximately aligns with one of the two  $\sigma_v$  planes of the Pc unit (Fig. 1). This effectively tilts the Pc group to one side, hence breaking the equivalency of pyrrolic units, in line with the low symmetry observed by NMR of the Y derivative.

10

15

20

25

30

35

40

45

50

The electronic absorption spectra of 1, 2 and 3 in CH<sub>2</sub>Cl<sub>2</sub> exhibit a typical Soret band at ~352 nm and an intense Q-band at ~693 and ~710 nm (Fig. S8†). This splitting of the Q-band, similar to other heteroleptic bis(phthalocyanato) LnIII complexes, arises due to lowered molecular symmetry resulting in different possible transitions. 20,47-49 In addition to the Soret and Q-bands of Pc ligand origin, the spectra display another band at ~260 nm corresponding to an O → W charge transfer transition in the PW<sub>11</sub>O<sub>39</sub> unit. FT-IR spectra of 1, 2 and 3 (Fig. S6 and S7†) display vibrations related to  $\nu$ (C-H)  $\sim 2960-2853 \text{ cm}^{-1}$ ,  $\nu(C=N) \sim 1632 \text{ cm}^{-1}$ ,  $\delta(CH_2) \sim 1458 \text{ cm}^{-1}$ ,  $\nu(\mbox{P-O}) \sim \!\! 1094$  and 1056  $\mbox{cm}^{-1},\, \nu(\mbox{W-O}_{\rm terminal}) \sim \!\! 953~\mbox{cm}^{-1},\, \nu(\mbox{W-O}_{\rm terminal})$ O<sub>b</sub>-W) ~886 cm<sup>-1</sup> (bridging oxygen of two octahedral W sharing a corner) and  $\nu(W-O_c-W)$  800-730 cm<sup>-1</sup> (bridging oxygen of two octahedral W sharing an edge). ESI-HRMS in the negative mode for 1, 2 and 3 show fragmentations characteristic for the triply negatively charged species [M + NBu<sub>4</sub> +

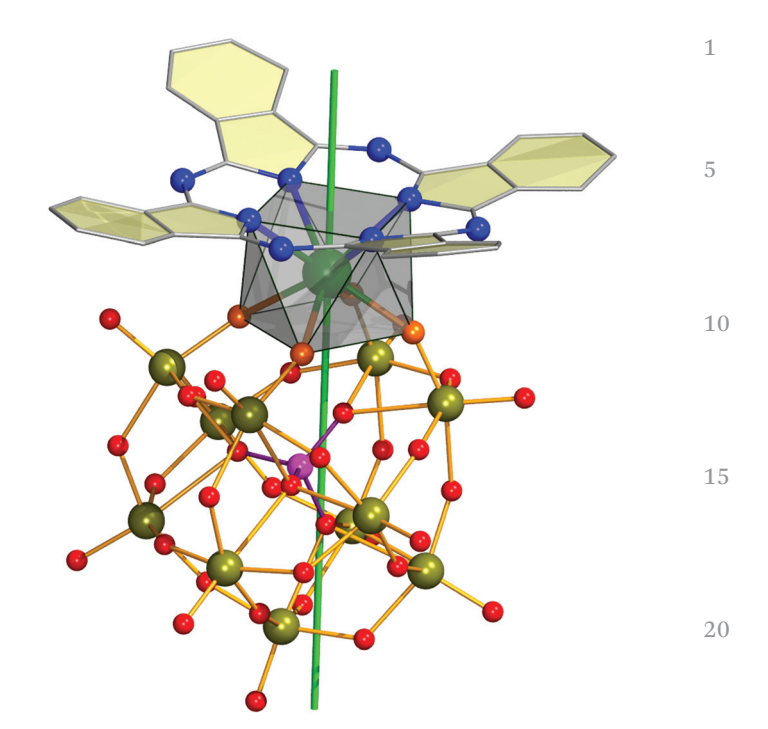


Fig. 1 Molecular structure of the  $[Y^{III}(Pc)(PW_{11}O_{39})]^{6}$ -anion in 1. The distorted square-antiprismatic  $YN_4O_4$  coordination polyhedron is highlighted in transparent grey, and the orientation of its associated local  $C_4$  axis is shown as green line. The four oxygen centres surrounding the lacunary site of the  $[PW_{11}O_{39}]^{7}$ - group, to which the  $Y^{3+}$  ion coordinates, are shown in orange. Colour code: Y: green, W: dark yellow, P: purple, O: red, N: blue, C: light grey. H atoms omitted for clarity. Benzene and pyrrole rings of the Pc ligand are shown in transparent yellow to better illustrate the bent Pc geometry.

25

30

35

2H]<sup>3-</sup> and [M +  $2NBu_4$  + H]<sup>3-</sup>, where M = [Ln<sup>III</sup>(Pc) ( $PW_{11}O_{39}$ )]<sup>6-</sup>. The isotopic distributions of the calculated species perfectly match with m/z deviations within  $\sim 0.0005$  and  $\sim 0.0004$ , respectively (Fig. 2b, S4 and 5†).

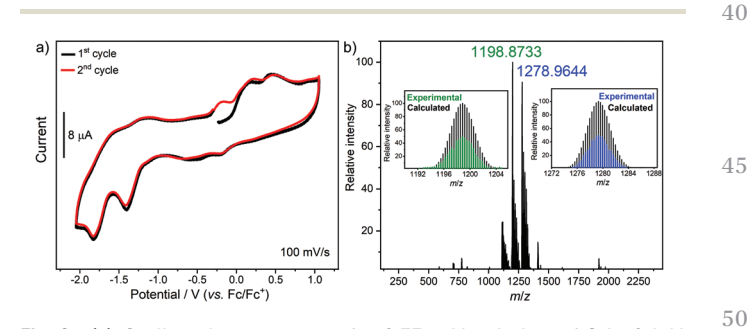


Fig. 2 (a) Cyclic voltammogram of a 0.33 mM solution of 2 in 0.1 M NBu<sub>4</sub>PF<sub>6</sub> in CH<sub>2</sub>Cl<sub>2</sub>. Sweeping direction is from negative to positive potentials. (b) Full ESI-HRMS spectrum of 2, M = [Dylll(Pc)(PW<sub>11</sub>O<sub>39</sub>)]<sup>6-</sup>. The inset shows the partial ESI-HRMS corresponding to [M + NBu<sub>4</sub> + 2H]<sup>3-</sup> = [C<sub>48</sub>H<sub>54</sub>N<sub>9</sub>O<sub>39</sub>PW<sub>11</sub>Dy]<sup>3-</sup> (green) and [M + 2NBu<sub>4</sub> + H]<sup>3-</sup> = [C<sub>64</sub>H<sub>89</sub>N<sub>10</sub>O<sub>39</sub>PW<sub>11</sub>Dy]<sup>3-</sup> (blue), compared to calculated isotopic distribution (black), corresponding to m/z = 1198.8732 and 1278.9649, respectively. Experimental and theoretical relative abundances have been adjusted to 50% and 100%, respectively, for the purpose of comparison.

Dalton Transactions Communication

Cyclic voltammograms of 1, 2 and 3 were performed in 10 mL CH<sub>2</sub>Cl<sub>2</sub> solutions using [NBu<sub>4</sub>][PF<sub>6</sub>] (0.1 M) as electrolyte, a glassy carbon working electrode, and a Pt wire as reference and counter electrode. All complexes show similar behaviour (Fig. 2a and S3†). Plotted data were corrected for ohmic drop (PEIS method) and referenced vs.  $[Cp_2Fe]/[Cp_2Fe]^+$ . The CVs do not display any marked redox couples, and except for the reduction potentials at  $E_{\rm pc} \sim -1.80$  V and  $E_{\rm pc} \sim -1.40$  V, the oxidation and reduction processes are not well defined. Electrochemistry of complexes containing Pc ligands show multiple redox couples based on oxidation and reduction of the Pc ring. 50-52 The  $\left[PW_{11}O_{39}\right]^{7-}$  constituent is only redoxactive at negative potentials showing a quasi-reversible couple  $W^{VI}/W^{V}$  at  $E_{1/2} = -1.18 \text{ V (Fig. S2}^{\dagger})$ . Therefore, by comparison with the starting materials, oxidation peaks at  $\sim$ -1.58,  $\sim$ +0.18 and ~+0.46 V and reduction peaks at ~-1.80 V are associated to Pc. Meanwhile, the observed  $E_{\rm pc} \sim -1.40$  V and  $E_{\rm pa} \sim -1.20$ V are likely overlapping redox processes occurring in both the Pc ligand and POM unit. Narrowing the window of the sweeping potential in the negative (-2.10 V to -0.24 V) and positive (-0.25 V to +0.94 V) ranges yielded identical features to the full spectra (Fig. S1†). Thermogravimetric analysis (TGA) of 1, 2 and 3 (Fig. S9†) exhibit thermal stability until 200 °C, and up to ca. 400 °C the complexes lose all NBu<sub>4</sub> countercations (ca. 22%).

10

15

20

25

30

40

45

50

Direct current (dc) magnetic susceptibility and magnetisation data for 2 and 3 are shown in Fig. 3a as  $\chi_{\rm m} T \, \nu s. \, T$  at 0.1 T

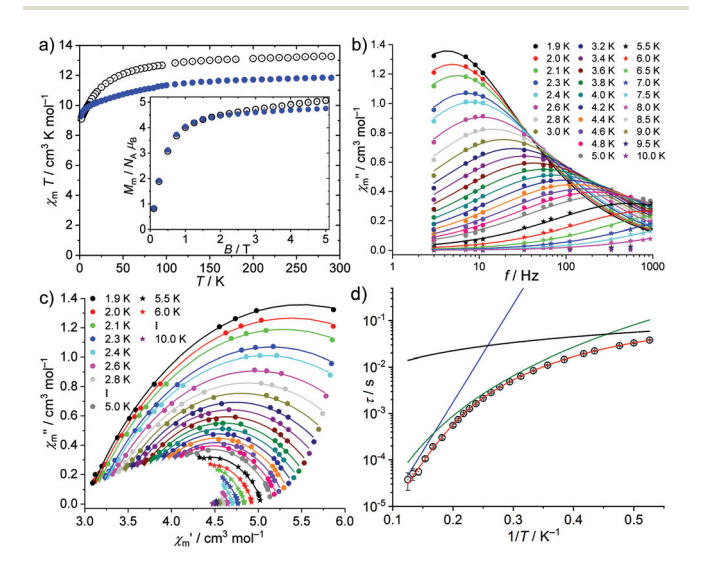


Fig. 3 (a) Dc data:  $\chi_m T$  vs. T at 0.1 T and  $M_m$  vs. B at 2.0 K (inset) for 2 (black open circles) and 3 (blue full circles; because of the loss of lattice solvent during the treatment of the sample, leading to uncertainty in the molar mass, the  $\chi_m T$  at 290 K was scaled to 11.84 cm³ K mol<sup>-1</sup>). (b) Outof-phase molar magnetic susceptibility  $\chi''_m$  vs. f for 2 (symbols: data, lines: fits to generalised Debye expression). (c) Magnetic ac data for 2: Cole–Cole plot in the range 1.9–10.0 K at a static bias field of 500 Oe (symbols: data, lines: fits to a generalised Debye expression). (d) Arrhenius plot of relaxation time  $\tau$  vs.  $T^{-1}$  (1.9 K  $\leq T \leq$  8.0 K) for 2, red line shows a combined fit to Orbach (blue), Raman (green) and direct relaxation (black) processes.

and  $M_{\rm m}$  vs. B at 2.0 K. At 290 K, the  $\chi_{\rm m}T$  values are 13.26 (2) and 11.84 cm3 K mol-1 (3), in good agreement with those expected for an isolated Dy<sup>III</sup> or Tb<sup>III</sup> centre (Dy<sup>III</sup>: 13.01-14.05 cm<sup>3</sup> K mol<sup>-1</sup>, Tb<sup>III</sup>: 11.76-12.01 cm<sup>3</sup> K mol<sup>-1</sup>).<sup>53</sup> Upon cooling, the values of  $\chi_{\rm m}T$  gradually decrease to 12.63 (2) or 11.24 cm<sup>3</sup> K mol<sup>-1</sup> (3) at 90 K, and subsequently drop to reach 9.10 (2) or 9.31 cm<sup>3</sup> K mol<sup>-1</sup> (3) at 2.0 K. These drop-offs are due to the thermal depopulation of the energy states of the respective split ground terms <sup>6</sup>H<sub>15/2</sub> (Dy<sup>III</sup>) or <sup>7</sup>F<sub>6</sub> (Tb<sup>III</sup>). At 2.0 K, the molar magnetisation as a function of the applied magnetic field (Fig. 3a, inset) steeply rises at low fields (0-1 T) and slightly increases at higher fields reaching a value of 5.1 (2) or  $4.8N_A\mu_B$  (3) at 5.0 T. As expected, this value is about half of the saturation value of a single  $Dy^{III}$  (10 $N_A\mu_B$ ) or  $Tb^{III}$  $(9N_A\mu_B)$  centre, since these data represent the mean value of a statistical arrangement (i.e. powder sample) of magnetically anisotropic lanthanide centres.

For 3, weak out-of-phase ac susceptibility signals were detected at static bias fields above 100 Oe and below 1000 Oe. However, the curvature in the Cole-Cole plots (Fig. S16,† bottom) are not pronounced enough to obtain a reliable fit. For 2, weak out-of-phase signals were detected at zero static bias field (Fig. S16,† top-left). At a 500 Oe static bias field, optimal conditions for fitting the data were found, i.e. pronounced curvatures in the Cole-Cole plot (Fig. 3c) and maxima in the  $\chi''_{\rm m}$  vs. f representation (Fig. 3b). The data were analysed in terms of a generalised Debye expression<sup>54</sup> at each temperature yielding the lines in the Cole-Cole plot and  $(\chi'_m)$  $\chi''_{\rm m}$ ) vs. f plots, and the relaxation times  $\tau$  (Fig. 3d). The distribution of these relaxation times is  $\alpha = 0.383 \pm 0.052$ , suggesting multiple relaxation pathways. We therefore analysed the data shown in the Arrhenius plot considering numerous slow relaxation processes and found an adequate description by adopting Orbach, Raman and direct relaxation processes. The corresponding formula is given by  $\tau^{-1} = \tau_0^{-1} \exp(-\tau_0^{-1})$  $U_{\text{eff}}/k_{\text{B}}T$ ) +  $CT^{n}$  +  $A_{\text{K}}T$  ( $k_{\text{B}}$ : Boltzmann's constant). The leastsquares fit yields an attempt time  $\tau_0 = (1.08 \pm 0.31) \times 10^{-7}$  s and an effective barrier  $U_{\text{eff}} = (33.7 \pm 1.5) \text{ cm}^{-1}$  for the Orbach process, a constant  $C = (0.41 \pm 0.08) \text{ s}^{-1} \text{ K}^{-n}$  and an exponent n = 4.9  $\pm$  0.2 for the Raman process, and a constant  $A_{\rm K}$  = (8.9  $\pm$ 0.6)  $s^{-1} K^{-1}$  at 500 Oe static bias field for the direct process. The Orbach process parameters are in the common range of Dy<sup>III</sup> SIMs, <sup>10</sup> while the parameters for the Raman and direct processes are within the expected range for systems with closely spaced Kramers levels (n = 5). The corresponding homoleptic double-decker complexes, i.e. [DyIII(Pc)2] and  $[\mathrm{Dy^{III}}(\mathrm{PW_{11}O_{39}})_2]^{11-}$ , exhibit effective energy barriers  $U_{\mathrm{eff}} = 28$ and 38.2 cm $^{-1}$  and  $au_0$  values of 6.25 imes 10 $^{-6}$  and 9.6 imes 10 $^{-12}$  s respectively.  $^{15,56}$  The  $U_{\rm eff}$  value of 2 thus represents the average value, however, in contrast to  $[Dy^{III}(PW_{11}O_{39})_2]^{11-}$ , it shows a more pronounced curvature of the isotherms in the Cole-Cole plot (at a significantly smaller bias field; 500 Oe vs. 3000 Oe).

In conclusion, we have reported the synthesis and characterisation of a family of new hybrid complexes of formula  $[M^{III}(Pc)(PW_{11}O_{39})]^{6-}$ , formed by combining two tetradentate ligands with donor atoms forming  $O_4$  and  $N_4$  squares of nearly

2.5

40

Communication Dalton Transactions

identical size (ca. 2.8 Å side length), namely the polyoxotungstate  $[PW_{11}O_{39}]^{7-}$  and unsubstituted phthalocyanate. The observation of SMM behaviour in 2 will prompt further investigations into the derivatisation of the peripheral hydrogens on the Pc ligand (e.g. with electron-donating and electron-withdrawing groups) and the use of other lacunary POMs (Keggin and Wells–Dawson type) to study the magnetic response.

#### Conflicts of interest

10

25

30

35

40

45

There are no conflicts to declare.

## Acknowledgements

We thank the Punjab Educational Endowment Fund (PEEF) for Ms. Sidra Sarwar's CMMS Scholarship.

### Notes and references

‡ Crystal data 3:  $C_{76}H_{122}N_{12}O_{39}PW_{11}Tb\cdot6(CH_2Cl_2)\ M_r=4549.64\ g\ mol^{-1},$  monoclinic, C2/m (no. 12),  $a=22.5917(14)\ \mathring{A},\ b=21.7413(12)\ \mathring{A},\ c=26.2648(15)\ \mathring{A},\ \beta=95.3550(10)^\circ,\ \alpha=\gamma=90^\circ,\ V=12\ 844.3(13)\ \mathring{A}^3,\ T=100.15\ K,\ Z=4,\ Z'=0.5,\ \mu(\text{Synchrotron})=9.767,\ 53\ 920\ reflections\ measured,\ 7102\ unique\ (R_{\rm int}=0.0833)$  which were used in all calculations. The final  $wR_2$  was 0.1507 (all data) and  $R_1$  was 0.0509 (I>2(I)). CCDC 1993275.†

1:  $C_{192}H_{324}N_{24}O_{78}P_2W_{22}Y\cdot3.5(CH_2Cl_2)$ ,  $M_r=8798.43$  g mol<sup>-1</sup>, monoclinic,  $P2_1/c$  (No. 14), a=29.676(4) Å, b=30.709(4) Å, c=29.725(4) Å,  $\beta=91.830(2)^\circ$ ,  $\alpha=\gamma=90^\circ$ , V=27 074(5) ų, T=100.0 K, Z=4, Z'=1,  $\mu(\text{Synchrotron})=9.036$ , 213 327 reflections measured, 28 548 unique ( $R_{\text{int}}=0.1538$ ) which were used in all calculations. The final w $R_2$  was 0.2344 (all data) and  $R_1$  was 0.0869 (I>2(I)). CCDC 1993274.†

- 1 G. Christou, D. Gatteschi, D. N. Hendrickson and R. Sessoli, MRS Bull., 2000, 25, 66.
- 2 R. Sessoli, D. Gatteschi, A. Caneschi and M. Novak, *Nature*, 1993, **365**, 141.
- 3 L. Bogani and W. Wernsdorfer, Nat. Mater., 2008, 7, 179.
- 4 K. Katoh, H. Isshiki, T. Komeda and M. Yamashita, *Chem. Asian J.*, 2012, 7, 1154.
- 5 K. Katoh, H. Isshiki, T. Komeda and M. Yamashita, *Coord. Chem. Rev.*, 2011, **255**, 2124.
- 6 E. Moreno-Pineda, C. Godfrin, F. Balestro, W. Wernsdorfer and M. Ruben, *Chem. Soc. Rev.*, 2018, 47, 501.
- 7 A. Gaita-Ariño, F. Luis, S. Hill and E. Coronado, *Nat. Chem.*, 2019, 11, 301.
- 8 M. Urdampilleta, N.-V. Nguyen, J.-P. Cleuziou, S. Klyatskaya, M. Ruben and W. Wernsdorfer, *Int. J. Mol. Sci.*, 2011, **12**, 6656.
- 9 N. Ishikawa, M. Sugita and W. Wernsdorfer, *J. Am. Chem. Soc.*, 2005, 127, 3650.
- 10 D. N. Woodruff, R. E. P. Winpenny and R. A. Layfield, *Chem. Rev.*, 2013, **113**, 5110.
- 11 J. Luzon and R. Sessoli, Dalton Trans., 2012, 41, 13556.
- 12 J. D. Rinehart and J. R. Long, Chem. Sci., 2011, 2, 2078.
- 13 S. T. Liddle and J. van Slageren, *Chem. Soc. Rev.*, 2015, 44, 6655

14 J.-L. Liu, Y.-C. Chen and M.-L. Tong, Chem. Soc. Rev., 2018, 47, 2431.

- 15 N. Ishikawa, M. Sugita, T. Ishikawa, S.-Y. Koshihara and Y. Kaizu, *J. Am. Chem. Soc.*, 2003, 125, 8694.
- 16 S.-D. Jiang, B.-W. Wang, H.-L. Sun, Z.-M. Wang and S. Gao, *J. Am. Chem. Soc.*, 2011, **133**, 4730.
- 17 S. D. Jiang, B. W. Wang, G. Su, Z. M. Wang and S. Gao, *Angew. Chem.*, *Int. Ed.*, 2010, **49**, 7448.
- 18 L. Ungur, J. J. Le Roy, I. Korobkov, M. Murugesu and L. F. Chibotaru, *Angew. Chem., Int. Ed.*, 2014, 53, 4413.

10

15

20

2.5

30

40

45

50

55

- 19 M. Gonidec, F. Luis, A. Vílchez, J. Esquena, D. B. Amabilino and J. Veciana, *Angew. Chem., Int. Ed.*, 2010, **49**, 1623.
- 20 C. R. Ganivet, B. Ballesteros, G. de la Torre, J. M. Clemente-Juan, E. Coronado and T. Torres, *Chem. – Eur. J.*, 2013, **19**, 1457.
- 21 M. Gonidec, I. Krivokapic, J. Vidal-Gancedo, E. S. Davies, J. McMaster, S. M. Gorun and J. Veciana, *Inorg. Chem.*, 2013, 52, 4464.
- 22 H. Shang, S. Zeng, H. Wang, J. Dou and J. Jiang, *Sci. Rep.*, 2015, 5, 8838.
- 23 M. Gonidec, D. B. Amabilino and J. Veciana, *Dalton Trans.*, 2012, 41, 13632.
- 24 Y. Chen, F. Ma, X. Chen, B. Dong, K. Wang, S. Jiang, C. Wang, X. Chen, D. Qi and H. Sun, *Inorg. Chem. Front.*, 2017, 4, 1465.
- 25 Y. Chen, F. Ma, X. Chen, B. Dong, K. Wang, S. Jiang, C. Wang, X. Chen, D. Qi and H. Sun, *Inorg. Chem.*, 2017, 56, 13889.
- 26 F. Gao, Y.-Y. Li, C.-M. Liu, Y.-Z. Li and J.-L. Zuo, *Dalton Trans.*, 2013, **42**, 11043.
- 27 H. Ke, W. K. Wong, W. Y. Wong, H. L. Tam, C. T. Poon and F. Jiang, *Eur. J. Inorg. Chem.*, 2009, 2009, 1243.
- 28 F. Lu, X. Sun, R. Li, D. Liang, P. Zhu, C.-F. Choi, D. K. Ng, T. Fukuda, N. Kobayashi and M. Bai, *New J. Chem.*, 2004, 28, 1116.
- 29 F. Gao, X. Feng, L. Yang and X. Chen, *Dalton Trans.*, 2016, 45, 7476.
- 30 G. Lu, S. Yan, M. Shi, W. Yu, J. Li, W. Zhu, Z. Ou and K. M. Kadish, *Chem. Commun.*, 2015, 51, 2411.
- 31 H. Wang, K. Wang, J. Tao and J. Jiang, *Chem. Commun.*, 2012, **48**, 2973.
- 32 W. Cao, Y. Zhang, H. Wang, K. Wang and J. Jiang, *RSC Adv.*, 2015, **5**, 17732.
- 33 H. Wang, W. Cao, T. Liu, C. Duan and J. Jiang, *Chem. Eur. J.*, 2013, **19**, 2266.
- 34 W. Cao, C. Gao, Y.-Q. Zhang, D. Qi, T. Liu, K. Wang, C. Duan, S. Gao and J. Jiang, *Chem. Sci.*, 2015, **6**, 5947.
- 35 E. Coronado and C. J. Gomez-Garcia, Chem. Rev., 1998, 98, 273.
- 36 L. Ruhlmann and D. Schaming, *Trends in Polyoxometalates Research*, Nova Science Publishers, New York, 2015.
- 37 N. V. Izarova and P. Kögerler, in *Trends in Polyoxometalates Research*, ed. L. Ruhlmann and D. Schaming, Nova Science Publishers, New York, 2015, pp. 121–149.
- 38 Y.-F. Song, *Polyoxometalate-Based Assemblies and Functional Materials*, Springer International Publishing, 2018.
- 39 S.-S. Wang and G.-Y. Yang, Chem. Rev., 2015, 115, 4893.

Dalton Transactions Communication

40 K. Y. Monakhov, M. Moors and P. Kögerler, in Advances in 48 M. M. Ayhan, A. Singh, E. Jeanneau, V. Ahsen, J. Zyss, 1 Inorganic Chemistry, ed. R. van Eldik and L. Cronin, Academic I. Ledoux-Rak, A. G. Gürek, C. Hirel, Y. Bretonnière and Press, Elsevier, Amsterdam, 2017, vol. 69, pp. 251-286. C. Andraud, Inorg. Chem., 2014, 53, 4359. 41 J.-P. Wang, J.-W. Zhao, X.-Y. Duan and J.-Y. Niu, Cryst. 49 V. E. Pushkarev, V. V. Kalashnikov, A. Y. Tolbin, 5 5 Growth Des., 2006, 6, 507. S. A. Trashin, N. E. Borisova, S. V. Simonov, V. B. Rybakov, 42 S. Zhang, Y. Wang, J. Zhao, P. Ma, J. Wang and J. Niu, L. G. Tomilova and N. S. Zefirov, Dalton Trans., 2015, 44, Dalton Trans., 2012, 41, 3764. 16553. 43 K. Wang, D. Zhang, J. Ma, P. Ma, J. Niu and J. Wang, 50 P. Zhu, F. Lu, N. Pan, D. P. Arnold, S. Zhang and J. Jiang, CrystEngComm, 2012, 14, 3205. Eur. J. Inorg. Chem., 2004, 2004, 510. 10 10 44 H.-Y. Zhao, J.-W. Zhao, B.-F. Yang, H. He and G.-Y. Yang, 51 M. Arıcı, C. Bozoğlu, A. Erdoğmuş, A. L. Uğur and A. Koca, CrystEngComm, 2013, 15, 8186. Electrochim. Acta, 2013, 113, 668. 45 J. Iijima, H. Naruke and T. Sanji, RSC Adv., 2016, 6, 91494. 52 E. B. Orman, A. Koca, A. R. Özkaya, İ. Gürol, M. Durmus 46 R. Pütt, X. Qiu, P. Kozłowski, H. Gildenast, O. Linnenberg, and V. Ahsen, J. Electrochem. Soc., 2014, 161, H422. S. Zahn, R. Chiechi and K. Monakhov, Chem. Commun., 53 H. Lueken, Magnetochemie, Teubner, Stuttgart, 1999. 15 15 54 K. S. Cole and R. H. Cole, J. Chem. Phys., 1941, 9, 341. 2019, 55, 13554. 47 Y. Bian, R. Wang, D. Wang, P. Zhu, R. Li, J. Dou, W. Liu, 55 K. N. Shrivastava, Phys. Status Solidi B, 1983, 117, 437. C.-F. Choi, H.-S. Chan, C. Ma, D. K. P. Ng and J. Jiang, Helv. 56 P. Ma, F. Hu, Y. Huo, D. Zhang, C. Zhang, J. Niu and Chim. Acta, 2004, 87, 2581. J. Wang, Cryst. Growth Des., 2017, 17, 1947. 20 20 25 25 30 30 35 35 40 40 45 45 50 50 55 55